

Robust H_∞ Coherent-Classical Estimation of Linear Quantum Systems

Shibdas Roy* and Ian R. Petersen

Abstract— We study robust H_∞ coherent-classical estimation for a class of physically realizable linear quantum systems with parameter uncertainties. Such a robust coherent-classical estimator, with or without coherent feedback, can yield better disturbance-to-error performance than the corresponding robust purely-classical estimator for an uncertain plant. Moreover, coherent feedback allows for such a robust coherent-classical estimator to be more robust to uncertainty in comparison to the robust classical-only estimator.

I. INTRODUCTION

It has been of significant interest recently to study estimation and control problems for quantum systems [1]–[5]. Linear quantum systems [1]–[4], [6], [7] are an important class of quantum systems, and allow for describing quantum optical devices such as finite bandwidth squeezers [7], optical cavities [6], and linear quantum amplifiers [7]. Coherent feedback control for linear quantum systems, where the feedback controller is also a quantum system, has been more recently studied [3]–[5]. A related coherent-classical estimation problem has been considered by the authors in [8]–[10], where the estimator consists of a classical part, which produces the desired final estimate and a quantum part, which may also involve coherent feedback. A quantum observer, as constructed in [2], is a purely quantum system, that produces a quantum estimate of a variable for the quantum plant. In contrast, a coherent-classical estimator is a mixed quantum-classical system, that produces a classical estimate of a variable for the quantum plant.

The authors have previously studied robust H_∞ classical estimation for an uncertain linear quantum system [11]. In this paper, we apply and extend such a robust H_∞ estimator to the problem of coherent-classical estimation of an uncertain quantum plant. We note that for a suitable choice of the coherent controller, a robust H_∞ coherent-classical estimator may yield improved disturbance attenuation when compared to the classical-only estimation scheme of [11]. Furthermore, we observe that with the addition of coherent feedback from the controller to the plant, such a robust H_∞ coherent-classical estimator exhibits superior robustness to uncertainty than the purely-classical robust H_∞ estimator.

II. ROBUST PURELY-CLASSICAL ESTIMATION

A schematic diagram of a classical estimation scheme is provided in Fig. 1. The quantum plant is defined as linear

This work was supported by the Australian Research Council and the Singapore National Research Foundation.

S. Roy is with the Department of Electrical and Computer Engineering, National University of Singapore, Singapore, and I. R. Petersen is with the School of Engineering and Information Technology, University of New South Wales, Canberra, Australia.

*roy_shibdas at yahoo.co.in

quantum stochastic differential equations (QSDEs) [9]:

$$\begin{aligned} \begin{bmatrix} da(t) \\ da(t)^\# \end{bmatrix} &= A \begin{bmatrix} a(t) \\ a(t)^\# \end{bmatrix} dt + B \begin{bmatrix} d\mathcal{A}(t) \\ d\mathcal{A}(t)^\# \end{bmatrix}, \\ \begin{bmatrix} d\mathcal{Y}(t) \\ d\mathcal{Y}(t)^\# \end{bmatrix} &= C \begin{bmatrix} a(t) \\ a(t)^\# \end{bmatrix} dt + D \begin{bmatrix} d\mathcal{A}(t) \\ d\mathcal{A}(t)^\# \end{bmatrix}, \\ z &= L \begin{bmatrix} a(t) \\ a(t)^\# \end{bmatrix}, \end{aligned} \quad (1)$$

$$\text{where } \begin{aligned} A &= \Omega(A_1, A_2), & B &= \Omega(B_1, B_2), \\ C &= \Omega(C_1, C_2), & D &= \Omega(D_1, D_2). \end{aligned} \quad (2)$$

Here, $a(t) = [a_1(t) \dots a_n(t)]^T$ is a vector of annihilation operators. The vector $\mathcal{A}(t) = [\mathcal{A}_1(t) \dots \mathcal{A}_m(t)]^T$ represents a collection of external independent quantum field operators and the vector $\mathcal{Y}(t)$ represents the corresponding vector of output field operators. Also, z denotes a scalar operator on the underlying Hilbert space and represents the quantity to be estimated. The notation $\Omega(A_1, A_2)$ denotes the matrix $\begin{bmatrix} A_1 & A_2 \\ A_2^\# & A_1^\# \end{bmatrix}$. Moreover, $A_1, A_2 \in \mathbb{C}^{n \times n}$, $B_1, B_2 \in \mathbb{C}^{n \times m}$, $C_1, C_2 \in \mathbb{C}^{m \times n}$, and $D_1, D_2 \in \mathbb{C}^{m \times m}$. Furthermore, $\#$ denotes the adjoint of a vector of operators or the complex conjugate of a complex matrix, and \dagger denotes the adjoint transpose of a vector of operators or the complex conjugate transpose of a complex matrix.

A linear quantum system of the form (1) should satisfy certain physical realizability conditions (See [8]–[10]) to represent an actual physical system. A quadrature of each (coherent) component of $\mathcal{Y}(t)$ is measured using homodyne detection to yield a corresponding classical signal y_i [8]:

$$\begin{aligned} dy_1 &= \frac{e^{-i\theta_1}}{\sqrt{2}} d\mathcal{Y}_1 + \frac{e^{i\theta_1}}{\sqrt{2}} d\mathcal{Y}_1^*, \\ &\vdots \end{aligned} \quad (3)$$

$$dy_m = \frac{e^{-i\theta_m}}{\sqrt{2}} d\mathcal{Y}_m + \frac{e^{i\theta_m}}{\sqrt{2}} d\mathcal{Y}_m^*.$$

Here, $\iota = \sqrt{-1}$, and $\theta_1, \dots, \theta_m$ determine the quadrature measured by each homodyne detector. The vector of signals $y = [y_1 \dots y_m]^T$ is then input to a classical estimator.

Corresponding to the system described by (1), (3), we define our uncertain system modelled as follows [11]:

$$\begin{aligned} \dot{x}(t) &= [A + \Delta A(t)]x(t) + [B + \Delta B(t)]w(t), \\ z(t) &= Lx(t), \\ y'(t) &= S[C + \Delta C(t)]x(t) + SDw(t), \end{aligned} \quad (4)$$

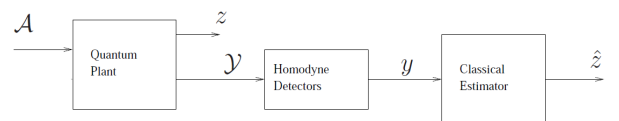


Fig. 1. Schematic diagram of classical estimation for a quantum plant.

where $x(t) := [a(t)^T \ a(t)^\dagger]^T$ is the state, $w(t)$ is the disturbance input, $z(t)$ is a linear combination of the state variables to be estimated, $y'(t)$ is the measured output, $L \in \mathbb{C}^{p \times 2n}$, $SC \in \mathbb{C}^{m \times 2n}$, $SD \in \mathbb{C}^{m \times 2m}$, $S = [S_1 \ S_2]$,

$$S_1 = \begin{bmatrix} \frac{e^{-\iota\theta_1}}{\sqrt{2}} & 0 & \dots & 0 \\ 0 & \frac{e^{-\iota\theta_2}}{\sqrt{2}} & \dots & 0 \\ & & \ddots & \\ & & & \frac{e^{-\iota\theta_m}}{\sqrt{2}} \end{bmatrix}, \quad (5)$$

$$S_2 = \begin{bmatrix} \frac{e^{\iota\theta_1}}{\sqrt{2}} & 0 & \dots & 0 \\ 0 & \frac{e^{\iota\theta_2}}{\sqrt{2}} & \dots & 0 \\ & & \ddots & \\ & & & \frac{e^{\iota\theta_m}}{\sqrt{2}} \end{bmatrix},$$

and $\Delta A(\cdot)$, $\Delta B(\cdot)$ and $\Delta C(\cdot)$ denote the time-varying parameter uncertainties, that have the following structure:

$$\begin{bmatrix} \Delta A(t) \\ \Delta C(t) \end{bmatrix} = \begin{bmatrix} H_1 \\ H_3 \end{bmatrix} F_1(t)E, \quad (6)$$

$$\Delta B(t) = H_2 F_2(t)G,$$

where H_1 , H_2 , H_3 , E and G are known complex constant matrices with appropriate dimensions, and the unknown matrix functions $F_1(\cdot)$ and $F_2(\cdot)$ satisfy the following bounds:

$$F_1^\dagger(t)F_1(t) \leq I, \quad F_2^\dagger(t)F_2(t) \leq I, \quad \forall t. \quad (7)$$

In addition, the uncertainties $\Delta A(t)$, $\Delta B(t)$ and $\Delta C(t)$ should satisfy certain constraints for the uncertain system (4) to be physically realizable (See [11]).

The robust H_∞ estimation problem for the uncertain system (4) can be converted into a scaled H_∞ control problem, similar to [12], by introducing the following parameterized linear time-invariant system corresponding to (4) [11]:

$$\begin{aligned} \dot{x}(t) &= Ax(t) + \begin{bmatrix} B & \frac{\gamma}{\epsilon_1}H_1 & \frac{\gamma}{\epsilon_2}H_2 \end{bmatrix} \tilde{w}(t), \\ \tilde{z}(t) &= \begin{bmatrix} \epsilon_1 E \\ 0 \\ L \end{bmatrix} x(t) + \begin{bmatrix} 0 & 0 & 0 \\ \epsilon_2 G & 0 & 0 \\ 0 & 0 & 0 \end{bmatrix} \tilde{w}(t) + \begin{bmatrix} 0 \\ 0 \\ -I \end{bmatrix} u(t), \\ y'(t) &= SCx(t) + \begin{bmatrix} SD & \frac{\gamma}{\epsilon_1}SH_3 & 0 \end{bmatrix} \tilde{w}(t). \end{aligned} \quad (8)$$

Here, $u(t)$ is the control input, $\tilde{z}(t)$ is the controlled output, $\epsilon_1, \epsilon_2 > 0$ are suitably chosen scaling parameters and $\gamma > 0$ is the desired level of disturbance attenuation for the robust H_∞ estimation problem. We also have the augmented disturbance $\tilde{w}(t) := [w(t)^T \ \frac{\epsilon_1}{\gamma}\eta(t)^T \ \frac{\epsilon_2}{\gamma}\xi(t)^T]^T$, where $\eta(t) := F_1(t)Ex(t)$, and $\xi(t) := F_2(t)Gw(t)$.

Theorem 1: (See [11]) Consider the robust H_∞ estimation problem for the uncertain system (4) converted to a scaled H_∞ control problem for the system (8). Given a prescribed level of disturbance attenuation $\gamma > 0$, a robust H_∞ estimator for the uncertain system (4) can be constructed, for some $\epsilon_1, \epsilon_2 > 0$, by solving the following two algebraic Riccati equations (AREs):

$$\begin{aligned} \bar{A}^\dagger X + X\bar{A} + X(\gamma^{-2}\bar{B}_1\bar{B}_1^\dagger)X \\ + \bar{C}_1^\dagger(I - \bar{D}_{12}\bar{E}_1^{-1}\bar{D}_{12}^\dagger)\bar{C}_1 = 0. \end{aligned} \quad (9)$$

$$\begin{aligned} \bar{A}Y + Y\bar{A}^\dagger + Y\bar{C}_1^\dagger\bar{C}_1Y + \gamma^{-2}\bar{B}_1\bar{B}_1^\dagger \\ - (\gamma^{-1}\bar{B}_1\bar{D}_{21}^\dagger + \gamma Y\bar{C}_2^\dagger) \\ \times \bar{S}^\dagger\bar{E}_2^{-1}\bar{S}(\gamma^{-1}\bar{B}_1\bar{D}_{21}^\dagger + \gamma Y\bar{C}_2^\dagger)^\dagger = 0. \end{aligned} \quad (10)$$

where

$$\begin{aligned} \bar{A} &= A, \quad \bar{C}_2 = C, \quad \bar{S} = S, \\ \bar{B}_1 &= \begin{bmatrix} B(I - \epsilon_2^2 G^\dagger G)^{-1/2} & \frac{\gamma}{\epsilon_1}H_1 & \frac{\gamma}{\epsilon_2}H_2 \end{bmatrix}, \\ \bar{C}_1 &= \begin{bmatrix} \epsilon_1 E \\ 0 \\ L \end{bmatrix}, \quad \bar{D}_{12} = \begin{bmatrix} 0 \\ 0 \\ -I \end{bmatrix}, \\ \bar{D}_{21} &= \begin{bmatrix} D(I - \epsilon_2^2 G^\dagger G)^{-1/2} & \frac{\gamma}{\epsilon_1}H_3 & 0 \end{bmatrix}, \\ \bar{E}_1 &= \bar{D}_{12}^\dagger\bar{D}_{12} = I, \\ \bar{E}_2 &= SD(I - \epsilon_2^2 G^\dagger G)^{-1}D^\dagger S^\dagger + \frac{\gamma^2}{\epsilon_1^2}SH_3H_3^\dagger S^\dagger. \end{aligned} \quad (11)$$

A suitable estimator is then given by:

$$\begin{aligned} \hat{x}(t) &= A_K \hat{x}(t) + B_K y'(t), \\ \hat{z}(t) &= C_K \hat{x}(t), \end{aligned} \quad (12)$$

where

$$\begin{aligned} A_K &= \bar{A} - B_K \bar{S} \bar{C}_2 + \gamma^{-2}(\bar{B}_1 - B_K \bar{S} \bar{D}_{21})\bar{B}_1^\dagger X, \\ B_K &= \gamma^2(I - YX)^{-1}(Y\bar{C}_2^\dagger\bar{S}^\dagger + \gamma^{-2}\bar{B}_1\bar{D}_{21}^\dagger\bar{S}^\dagger)\bar{E}_2^{-1}, \\ C_K &= -\bar{E}_1^{-1}\bar{D}_{12}^\dagger\bar{C}_1. \end{aligned} \quad (13)$$

The estimation error is given as:

$$e(t) := \hat{z}(t) - z(t) = C_K \hat{x}(t) - Lx(t). \quad (14)$$

Then, the disturbance-to-error transfer function is [11]:

$$\begin{aligned} \tilde{G}_{we}(s) &:= \frac{e(s)}{w(s)} = \begin{bmatrix} -L & C_K \end{bmatrix} \\ &\times \left(sI - \begin{bmatrix} A + \Delta A(t) & 0 \\ B_K S(C + \Delta C(t)) & A_K \end{bmatrix} \right)^{-1} \\ &\times \begin{bmatrix} B + \Delta B(t) \\ B_K SD \end{bmatrix}. \end{aligned} \quad (15)$$

We are interested in the disturbance \mathcal{A} to error e transfer function, which is simply the first component of the matrix transfer function $\tilde{G}_{we}(s)$. We shall ignore the other component, which is the disturbance $\mathcal{A}^\#$ to error e transfer function.

III. ROBUST COHERENT-CLASSICAL ESTIMATION

A schematic diagram of the coherent-classical estimation scheme is provided in Fig. 2. In this case, the plant output $\mathcal{Y}(t)$ does not directly drive a bank of homodyne detectors as in (3). Rather, this output is fed into another quantum system called a coherent controller, defined as [9]:

$$\begin{aligned} \begin{bmatrix} da_c(t) \\ da_c(t)^\# \end{bmatrix} &= A_c \begin{bmatrix} a_c(t) \\ a_c(t)^\# \end{bmatrix} dt + B_c \begin{bmatrix} d\mathcal{Y}(t) \\ d\mathcal{Y}(t)^\# \end{bmatrix}, \\ \begin{bmatrix} d\tilde{\mathcal{Y}}(t) \\ d\tilde{\mathcal{Y}}(t)^\# \end{bmatrix} &= C_c \begin{bmatrix} a_c(t) \\ a_c(t)^\# \end{bmatrix} dt + D_c \begin{bmatrix} d\mathcal{Y}(t) \\ d\mathcal{Y}(t)^\# \end{bmatrix}. \end{aligned} \quad (16)$$

A quadrature of each component of $\tilde{\mathcal{Y}}(t)$ is homodyne detected to produce a corresponding classical signal \tilde{y}_i [9]:

$$\begin{aligned} d\tilde{y}_1 &= \frac{e^{-\iota\theta_1}}{\sqrt{2}} d\tilde{\mathcal{Y}}_1 + \frac{e^{\iota\theta_1}}{\sqrt{2}} d\tilde{\mathcal{Y}}_1^*, \\ &\vdots \\ d\tilde{y}_{\tilde{m}} &= \frac{e^{-\iota\tilde{\theta}_{\tilde{m}}}}{\sqrt{2}} d\tilde{\mathcal{Y}}_{\tilde{m}} + \frac{e^{\iota\tilde{\theta}_{\tilde{m}}}}{\sqrt{2}} d\tilde{\mathcal{Y}}_{\tilde{m}}^*. \end{aligned} \quad (17)$$

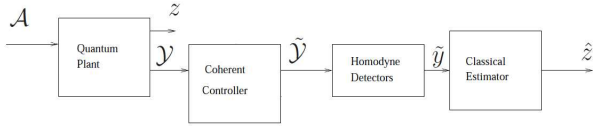


Fig. 2. Schematic diagram of coherent-classical estimation.

Here, the angles $\tilde{\theta}_1, \dots, \tilde{\theta}_{\tilde{m}}$ determine the quadrature measured by each homodyne detector. The vector of classical signals $\tilde{y} = [\tilde{y}_1 \dots \tilde{y}_{\tilde{m}}]^T$ is then used as the input to a robust H_∞ classical estimator of the form in the previous section.

The quantum plant (1) augmented with the coherent controller (16) is defined by the QSDEs [9]:

$$\begin{aligned} \begin{bmatrix} da(t) \\ da(t)^\# \\ da_c(t) \\ da_c(t)^\# \end{bmatrix} &= \begin{bmatrix} A & 0 \\ B_c C & A_c \end{bmatrix} \begin{bmatrix} a(t) \\ a(t)^\# \\ a_c(t) \\ a_c(t)^\# \end{bmatrix} dt \\ &+ \begin{bmatrix} B \\ B_c D \end{bmatrix} \begin{bmatrix} dA(t) \\ dA(t)^\# \end{bmatrix}, \\ \begin{bmatrix} d\tilde{Y}(t) \\ d\tilde{Y}(t)^\# \end{bmatrix} &= \begin{bmatrix} D_c C & C_c \end{bmatrix} \begin{bmatrix} a(t) \\ a(t)^\# \\ a_c(t) \\ a_c(t)^\# \end{bmatrix} dt \\ &+ D_c D \begin{bmatrix} dA(t) \\ dA(t)^\# \end{bmatrix}. \end{aligned} \quad (18)$$

The system (18) along with (17) is of the form:

$$\begin{aligned} \dot{x}_a(t) &= A_a x_a(t) + B_a w(t), \\ \tilde{y}'(t) &= S_a C_a x_a(t) + S_a D_a w(t), \end{aligned} \quad (19)$$

where $x_a(t) = [a(t)^T \ a(t)^\dagger \ a_c(t)^T \ a_c(t)^\dagger]^T$, $\tilde{y}'(t)$ is the measured output and

$$\begin{aligned} A_a &= \begin{bmatrix} A & 0 \\ B_c C & A_c \end{bmatrix}, B_a = \begin{bmatrix} B \\ B_c D \end{bmatrix}, \\ C_a &= \begin{bmatrix} D_c C & C_c \end{bmatrix}, D_a = D_c D, S_a = [\tilde{S}_1 \ \tilde{S}_2], \\ \tilde{S}_1 &= \begin{bmatrix} \frac{e^{-i\tilde{\theta}_1}}{\sqrt{2}} & 0 & \dots & 0 \\ 0 & \frac{e^{-i\tilde{\theta}_2}}{\sqrt{2}} & \dots & 0 \\ & & \ddots & \\ & & & \frac{e^{-i\tilde{\theta}_{\tilde{m}}}}{\sqrt{2}} \end{bmatrix}, \\ \tilde{S}_2 &= \begin{bmatrix} \frac{e^{i\tilde{\theta}_1}}{\sqrt{2}} & 0 & \dots & 0 \\ 0 & \frac{e^{i\tilde{\theta}_2}}{\sqrt{2}} & \dots & 0 \\ & & \ddots & \\ & & & \frac{e^{i\tilde{\theta}_{\tilde{m}}}}{\sqrt{2}} \end{bmatrix}. \end{aligned} \quad (20)$$

Let us now consider an uncertain plant of the form (4). Then the H_∞ estimation problem is for the following uncertain augmented system:

$$\begin{aligned} \dot{x}_a(t) &= [A_a + \Delta A_a(t)]x_a(t) + [B_a + \Delta B_a(t)]w(t), \\ z(t) &= L_a x_a(t), \\ \tilde{y}'(t) &= S_a [C_a + \Delta C_a(t)]x_a(t) + S_a D_a w(t), \end{aligned} \quad (21)$$

where we take $\Delta A_a(t) = H_{a1} F_1(t) E_a$, $\Delta B_a(t) = H_{a2} F_2(t) G_a$ and $\Delta C_a(t) = H_{a3} F_1(t) E_a$.

One can verify that these matrices can be expressed as:

$$\begin{aligned} H_{a1} &= \begin{bmatrix} H_1 \\ B_c H_3 \end{bmatrix}, H_{a2} = \begin{bmatrix} H_2 \\ 0 \end{bmatrix}, H_{a3} = D_c H_3, \\ E_a &= [E \ 0], G_a = G, L_a = [L \ 0]. \end{aligned} \quad (22)$$

The robust H_∞ estimator for the coherent-classical system is obtained by solving the following two AREs:

$$\begin{aligned} \bar{A}_a^\dagger X_a + X_a \bar{A}_a + X_a (\gamma^{-2} \bar{B}_{a1} \bar{B}_{a1}^\dagger) X_a \\ + \bar{C}_{a1}^\dagger (I - \bar{D}_{a12} \bar{E}_{a1}^{-1} \bar{D}_{a12}^\dagger) \bar{C}_{a1} = 0, \end{aligned} \quad (23)$$

$$\begin{aligned} \bar{A}_a Y_a + Y_a \bar{A}_a + Y_a \bar{C}_{a1}^\dagger \bar{C}_{a1} Y_a + \gamma^{-2} \bar{B}_{a1} \bar{B}_{a1}^\dagger \\ - (\gamma^{-1} \bar{B}_{a1} \bar{D}_{a21}^\dagger + \gamma Y_a \bar{C}_{a2}^\dagger) \\ \times \bar{S}_a^\dagger \bar{E}_2^{-1} \bar{S}_a (\gamma^{-1} \bar{B}_{a1} \bar{D}_{a21}^\dagger + \gamma Y_a \bar{C}_{a2}^\dagger)^\dagger = 0, \end{aligned} \quad (24)$$

which are of the forms (9) and (10), respectively.

Here, we have

$$\begin{aligned} \bar{A}_a &= A_a, \bar{C}_{a2} = C_a, \bar{S}_a = S_a, \\ \bar{B}_{a1} &= [B_a (I - \epsilon_2^2 G_a^\dagger G_a)^{-1/2} \ \frac{\gamma}{\epsilon_1} H_{a1} \ \frac{\gamma}{\epsilon_2} H_{a2}], \\ \bar{C}_{a1} &= \begin{bmatrix} \epsilon_1 E_a \\ 0 \\ L_a \end{bmatrix}, \bar{D}_{a12} = \begin{bmatrix} 0 \\ 0 \\ -I \end{bmatrix}, \\ \bar{D}_{a21} &= [D_a (I - \epsilon_2^2 G_a^\dagger G_a)^{-1/2} \ \frac{\gamma}{\epsilon_1} H_{a3} \ 0]. \end{aligned} \quad (25)$$

Then, a suitable robust estimator is given by

$$\begin{aligned} \dot{\hat{x}}_a(t) &= A_{aK} \hat{x}_a(t) + B_{aK} \tilde{y}'(t), \\ \hat{z}(t) &= C_{aK} \hat{x}_a(t), \end{aligned} \quad (26)$$

where

$$\begin{aligned} A_{aK} &= \bar{A}_a - B_{aK} \bar{S}_a \bar{C}_{a2} + \gamma^{-2} (\bar{B}_{a1} - B_{aK} \bar{S}_a \bar{D}_{a21}) \bar{B}_{a1}^\dagger X_a, \\ B_{aK} &= \gamma^2 (I - Y_a X_a)^{-1} (Y_a \bar{C}_{a2}^\dagger \bar{S}_a^\dagger + \gamma^{-2} \bar{B}_{a1} \bar{D}_{a21}^\dagger \bar{S}_a^\dagger) \bar{E}_{a2}^{-1}, \\ C_{aK} &= -\bar{E}_{a1}^{-1} \bar{D}_{a12}^\dagger \bar{C}_{a1}. \end{aligned} \quad (27)$$

Note that the matrices in (25) of the robust coherent-classical estimator can be expressed in terms of the corresponding matrices in (11) of the robust purely-classical estimator as follows:

$$\begin{aligned} \bar{A}_a &= \begin{bmatrix} \bar{A} & 0 \\ B_c \bar{C}_2 & A_c \end{bmatrix}, \bar{B}_{a1} = \begin{bmatrix} \bar{B}_1 \\ B_c \bar{D}_{21} \end{bmatrix}, \\ \bar{C}_{a1} &= [\bar{C}_1 \ 0], \bar{C}_{a2} = [D_c \bar{C}_2 \ C_c], \\ \bar{D}_{a12} &= \bar{D}_{12}, \bar{D}_{a21} = D_c \bar{D}_{21}. \end{aligned} \quad (28)$$

IV. NUMERICAL EXAMPLE

We now present a numerical example. A linear quantum system arising in quantum optics is a dynamic squeezer - an optical cavity with a non-linear active medium inside. Let the plant be a dynamic squeezer, described by [9]:

$$\begin{aligned} \begin{bmatrix} da \\ da^* \end{bmatrix} &= \begin{bmatrix} -\frac{\beta}{2} & -\chi \\ -\chi^* & -\frac{\beta}{2} \end{bmatrix} \begin{bmatrix} a \\ a^* \end{bmatrix} dt - \sqrt{\kappa} \begin{bmatrix} dA \\ dA^* \end{bmatrix}, \\ \begin{bmatrix} dY \\ dY^* \end{bmatrix} &= \sqrt{\kappa} \begin{bmatrix} a \\ a^* \end{bmatrix} dt + \begin{bmatrix} dA \\ dA^* \end{bmatrix}, \\ z(t) &= [0.1 \ -0.1] \begin{bmatrix} a \\ a^* \end{bmatrix}, \end{aligned} \quad (29)$$

where $\beta > 0$ is the overall cavity loss, $\kappa > 0$ determines the loss owing to the cavity mirrors, $\chi \in \mathbb{C}$ quantifies the non-linearity of the active medium, and a is a single annihilation operator of the cavity mode.

Here, we choose $\beta = 4$, $\kappa = 4$, and $\chi = 0.5$. These values are chosen arbitrarily for the purposes of demonstration of principle here, and may well represent actual practical values for the corresponding physical parameters. We ensure though that the quantum system is physically realizable, since we have $\beta = \kappa$ (See [8]–[10]). We fix the homodyne detection angle at 10° . Thus, the matrices in (1) may be obtained.

We introduce uncertainty in the parameter $\alpha := \sqrt{\kappa}$ as follows: $\alpha \rightarrow \alpha + \mu\delta(t)\alpha$, where $|\delta(t)| \leq 1$ is an uncertain parameter and $\mu \in [0, 1)$ is the level of uncertainty. Then,

$$\begin{aligned} \Delta A &= \begin{bmatrix} -\alpha^2\mu\delta - \frac{\alpha^2\mu^2\delta^2}{2} & 0 \\ 0 & -\alpha^2\mu\delta - \frac{\alpha^2\mu^2\delta^2}{2} \end{bmatrix}, \\ \Delta B &= \begin{bmatrix} -\mu\delta\alpha & 0 \\ 0 & -\mu\delta\alpha \end{bmatrix}, \Delta C = \begin{bmatrix} \mu\delta\alpha & 0 \\ 0 & \mu\delta\alpha \end{bmatrix}. \end{aligned} \quad (30)$$

We define the relevant matrices as follows:

$$\begin{aligned} F_1(t) &= \begin{bmatrix} \delta & 0 & 0 & 0 \\ 0 & \delta & 0 & 0 \\ 0 & 0 & \delta^2 & 0 \\ 0 & 0 & 0 & \delta^2 \end{bmatrix}, F_2(t) = \begin{bmatrix} \delta & 0 \\ 0 & \delta \end{bmatrix}, \\ E &= \begin{bmatrix} -\frac{1}{2} & 0 \\ 0 & -\frac{1}{2} \\ -\frac{1}{2} & 0 \\ 0 & -\frac{1}{2} \end{bmatrix}, G = \begin{bmatrix} 1 & 0 \\ 0 & 1 \end{bmatrix}, \\ H_1 &= \begin{bmatrix} 2\mu\alpha^2 & 0 & \mu^2\alpha^2 & 0 \\ 0 & 2\mu\alpha^2 & 0 & \mu^2\alpha^2 \end{bmatrix}, \\ H_2 &= \begin{bmatrix} -\mu\alpha & 0 \\ 0 & -\mu\alpha \end{bmatrix}, \\ H_3 &= \begin{bmatrix} -2\mu\alpha & 0 & 0 & 0 \\ 0 & -2\mu\alpha & 0 & 0 \end{bmatrix}. \end{aligned} \quad (31)$$

One can verify we have $\Delta A(t) = H_1 F_1(t) E$, $\Delta B(t) = H_2 F_2(t) G$ and $\Delta C(t) = H_3 F_1(t) E$, as required in (6). We fix $\delta = -1$, such that (7) is satisfied, and set $\mu = 0.1$.

We now solve the associated robust purely-classical H_∞ estimation problem using Theorem 1. We set $\gamma = 0.65$ and choose $\epsilon_1 = 0.19$, $\epsilon_2 = 0.81$, such that $\eta(t)$ and $\xi(t)$ are sufficiently suppressed, yielding satisfactory solutions to (9), (10). Then, an estimator is obtained as in (12) with:

$$\begin{aligned} A_K &= \begin{bmatrix} -0.0274 - 2.3799\iota & 1.8584 - 1.6718\iota \\ 1.8584 + 1.6718\iota & -0.0274 + 2.3799\iota \end{bmatrix}, \\ B_K &= \begin{bmatrix} -1.5600 + 1.5188\iota \\ -1.5600 - 1.5188\iota \end{bmatrix}, C_K = [0.1 \quad -0.1]. \end{aligned} \quad (32)$$

Now, let the controller be another dynamic squeezer [9]:

$$\begin{aligned} \begin{bmatrix} da_c \\ da_c^* \end{bmatrix} &= \begin{bmatrix} -\frac{\beta_c}{2} & -\chi_c \\ -\chi_c^* & -\frac{\beta_c}{2} \end{bmatrix} \begin{bmatrix} a_c \\ a_c^* \end{bmatrix} dt - \sqrt{\kappa_c} \begin{bmatrix} d\mathcal{Y} \\ d\mathcal{Y}^* \end{bmatrix}, \\ \begin{bmatrix} d\tilde{\mathcal{Y}} \\ d\tilde{\mathcal{Y}}^* \end{bmatrix} &= \sqrt{\kappa_c} \begin{bmatrix} a_c \\ a_c^* \end{bmatrix} dt + \begin{bmatrix} d\mathcal{Y} \\ d\mathcal{Y}^* \end{bmatrix}, \end{aligned} \quad (33)$$

where we choose $\beta_c = 4$, $\kappa_c = 4$, $\chi_c = -1$, such that it is physically realizable, and then obtain the matrices in (16).

We now consider the plant to be uncertain as in (30), (31). Also, we fix $\delta = -1$, $\mu = 0.1$ and the homodyne detection angle at 10° . We again set $\gamma = 0.65$, and choose

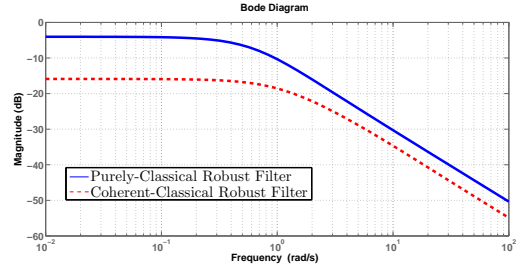


Fig. 3. Comparison of the estimation error frequency response of robust coherent-classical and robust purely-classical estimators.

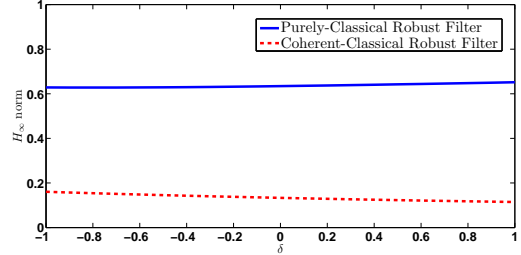


Fig. 4. Comparison of the H_∞ norm of the disturbance-to-error transfer functions for robust coherent-classical and robust purely-classical estimators.

$\epsilon_1 = 0.19$, $\epsilon_2 = 0.81$. A robust coherent-classical estimator is then obtained as in (26) with:

$$\begin{aligned} A_{aK} &= \begin{bmatrix} -2.03 + 0.13\iota & -0.86 + 0.03\iota & -0.28 + 0.14\iota & -0.31 + 0.03\iota \\ -0.86 - 0.03\iota & -2.03 - 0.13\iota & -0.31 - 0.03\iota & -0.28 - 0.14\iota \\ -6.59 + 0.50\iota & -2.90 - 0.47\iota & -4.95 + 0.54\iota & -1.95 - 0.50\iota \\ -2.90 + 0.47\iota & -6.59 - 0.50\iota & -1.95 + 0.50\iota & -4.95 - 0.54\iota \end{bmatrix}, \\ B_{aK} &= \begin{bmatrix} 0.21 - 0.06\iota \\ 0.21 + 0.06\iota \\ 2.12 - 0.01\iota \\ 2.12 + 0.01\iota \end{bmatrix}, C_{aK} = [0.1 \quad -0.1 \quad 0 \quad 0]. \end{aligned} \quad (34)$$

Fig. 3 shows a comparison of the error spectra (bode magnitude plots of the disturbance \mathcal{A} to error e transfer function only from (15) for augmented plant-controller system and plant alone respectively) of the robust coherent-classical filter and the robust purely-classical filter. Clearly, the robust H_∞ coherent-classical filter provides better disturbance attenuation compared to the robust H_∞ purely-classical filter. Fig. 4 shows a comparison of the H_∞ norm of the disturbance-to-error transfer functions as a function of $\delta \in [-1, 1]$ for the two robust filters. Clearly, the robust coherent-classical filter provides higher disturbance attenuation than the robust classical-only filter across the entire uncertainty window.

V. COHERENT FEEDBACK CASE

Here, we consider the case where there is quantum feedback from the controller to the plant [8], [10]. For this purpose, the plant is assumed to have an additional control

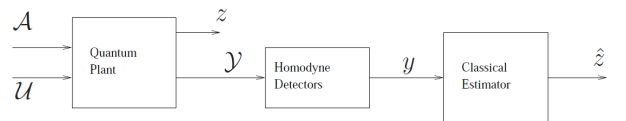


Fig. 5. Modified schematic diagram of purely-classical estimation.

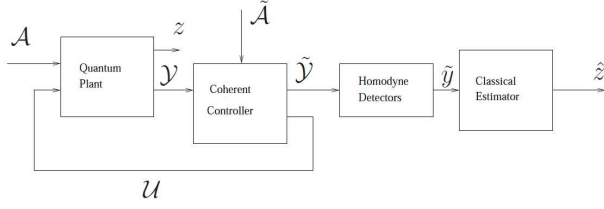


Fig. 6. Schematic of coherent-classical estimation with coherent feedback.

input \mathcal{U} (See Fig. 5). The plant (1) then is of the form [10]:

$$\begin{aligned} \begin{bmatrix} da(t) \\ da(t)^\# \end{bmatrix} &= A \begin{bmatrix} a(t) \\ a(t)^\# \end{bmatrix} dt + \begin{bmatrix} B_1 & B_2 \end{bmatrix} \begin{bmatrix} d\mathcal{A}(t) \\ d\mathcal{A}(t)^\# \\ d\mathcal{U}(t) \\ d\mathcal{U}(t)^\# \end{bmatrix}, \\ \begin{bmatrix} d\mathcal{Y}(t) \\ d\mathcal{Y}(t)^\# \end{bmatrix} &= C \begin{bmatrix} a(t) \\ a(t)^\# \end{bmatrix} dt + \begin{bmatrix} D & 0 \end{bmatrix} \begin{bmatrix} d\mathcal{A}(t) \\ d\mathcal{A}(t)^\# \\ d\mathcal{U}(t) \\ d\mathcal{U}(t)^\# \end{bmatrix}, \\ z &= L \begin{bmatrix} a(t) \\ a(t)^\# \end{bmatrix}. \end{aligned} \quad (35)$$

The uncertain plant along with (3) is then modelled as:

$$\begin{aligned} \dot{x}(t) &= [A + \Delta A(t)]x(t) + \begin{bmatrix} B_1 + \Delta B_1(t) & B_2 \end{bmatrix} \bar{w}(t), \\ z(t) &= Lx(t), \\ y'(t) &= S[C + \Delta C(t)]x(t) + S \begin{bmatrix} D & 0 \end{bmatrix} \bar{w}(t), \end{aligned} \quad (36)$$

where $\bar{w}(t) := [w(t)^T \ u_c(t)^T]^T$, and $u_c(t)$ is the spare control input. Also, we have $\Delta A(t) = H_1 F_1(t)E$, $\Delta B_1(t) = H_2 F_2(t)G$, $\Delta C(t) = H_3 F_1(t)E$. The robust purely-classical estimator is then obtained from Theorem 1, where we have:

$$\begin{aligned} \bar{A} &= A, \bar{C}_2 = C, \bar{S} = S, \\ \bar{B}_1 &= \begin{bmatrix} B_1(I - \epsilon_2^2 G^\dagger G)^{-1/2} & B_2 & \frac{\gamma}{\epsilon_1} H_1 & \frac{\gamma}{\epsilon_2} H_2 \end{bmatrix}, \\ \bar{C}_1 &= \begin{bmatrix} \epsilon_1 E \\ 0 \\ L \end{bmatrix}, \bar{D}_{12} = \begin{bmatrix} 0 \\ 0 \\ -I \end{bmatrix}, \\ \bar{D}_{21} &= \begin{bmatrix} D(I - \epsilon_2^2 G^\dagger G)^{-1/2} & 0 & \frac{\gamma}{\epsilon_1} H_3 & 0 \end{bmatrix}. \end{aligned} \quad (37)$$

The controller here would have an additional output that is fed back to the control input of the plant (See Fig. 6). The controller is defined as [8], [10]:

$$\begin{aligned} \begin{bmatrix} da_c(t) \\ da_c(t)^\# \end{bmatrix} &= A_c \begin{bmatrix} a_c(t) \\ a_c(t)^\# \end{bmatrix} dt \\ &+ \begin{bmatrix} B_{c1} & B_{c2} \end{bmatrix} \begin{bmatrix} d\tilde{\mathcal{A}}(t) \\ d\tilde{\mathcal{A}}(t)^\# \\ d\mathcal{Y}(t) \\ d\mathcal{Y}(t)^\# \end{bmatrix}, \\ \begin{bmatrix} d\tilde{\mathcal{Y}}(t) \\ d\tilde{\mathcal{Y}}(t)^\# \\ d\mathcal{U}(t) \\ d\mathcal{U}(t)^\# \end{bmatrix} &= \begin{bmatrix} \tilde{C}_c \\ C_c \end{bmatrix} \begin{bmatrix} a_c(t) \\ a_c(t)^\# \end{bmatrix} dt \\ &+ \begin{bmatrix} \tilde{D}_{c1} & \tilde{D}_{c2} \\ D_{c1} & D_{c2} \end{bmatrix} \begin{bmatrix} d\tilde{\mathcal{A}}(t) \\ d\tilde{\mathcal{A}}(t)^\# \\ d\mathcal{Y}(t) \\ d\mathcal{Y}(t)^\# \end{bmatrix}. \end{aligned} \quad (38)$$

The plant (35) and the controller (38) can be combined to yield an augmented system [8], [10]:

$$\begin{aligned} \begin{bmatrix} da(t) \\ da(t)^\# \\ da_c(t) \\ da_c(t)^\# \end{bmatrix} &= \begin{bmatrix} A + B_2 D_{c2} C & B_2 C_c \\ B_{c2} C & A_c \end{bmatrix} \begin{bmatrix} a(t) \\ a(t)^\# \\ a_c(t) \\ a_c(t)^\# \end{bmatrix} dt \\ &+ \begin{bmatrix} B_1 + B_2 D_{c2} D & B_2 D_{c1} \\ B_{c2} D & B_{c1} \end{bmatrix} \begin{bmatrix} d\mathcal{A}(t) \\ d\mathcal{A}(t)^\# \\ d\tilde{\mathcal{A}}(t) \\ d\tilde{\mathcal{A}}(t)^\# \end{bmatrix}, \\ \begin{bmatrix} d\tilde{\mathcal{Y}}(t) \\ d\tilde{\mathcal{Y}}(t)^\# \end{bmatrix} &= \begin{bmatrix} \tilde{D}_{c2} C & \tilde{C}_c \end{bmatrix} \begin{bmatrix} a(t) \\ a(t)^\# \\ a_c(t) \\ a_c(t)^\# \end{bmatrix} dt \\ &+ \begin{bmatrix} \tilde{D}_{c2} D & \tilde{D}_{c1} \end{bmatrix} \begin{bmatrix} d\mathcal{A}(t) \\ d\mathcal{A}(t)^\# \\ d\tilde{\mathcal{A}}(t) \\ d\tilde{\mathcal{A}}(t)^\# \end{bmatrix}. \end{aligned} \quad (39)$$

The augmented system (39) along with (17) is of the form (19), (20), with $w(t)$ replaced by $w'(t) := [d\mathcal{A}(t)^T \ d\mathcal{A}(t)^\dagger \ d\tilde{\mathcal{A}}(t)^T \ d\tilde{\mathcal{A}}(t)^\dagger]^T$, and with

$$\begin{aligned} A_a &= \begin{bmatrix} A + B_2 D_{c2} C & B_2 C_c \\ B_{c2} C & A_c \end{bmatrix}, \\ B_a &= \begin{bmatrix} B_1 + B_2 D_{c2} D & B_2 D_{c1} \\ B_{c2} D & B_{c1} \end{bmatrix}, \\ C_a &= [\tilde{D}_{c2} C \ \tilde{C}_c], \quad D_a = [\tilde{D}_{c2} D \ \tilde{D}_{c1}]. \end{aligned} \quad (40)$$

Let us now consider an uncertain plant of the form (36). Then the H_∞ estimation problem is considered for the following uncertain augmented system:

$$\begin{aligned} \dot{x}_a(t) &= [A_a + \Delta A_a(t)]x_a(t) + [B_a + \Delta B_a(t)]w'(t), \\ z(t) &= L_a x_a(t), \\ \tilde{y}'(t) &= S_a [C_a + \Delta C_a(t)]x_a(t) + S_a D_a w'(t), \end{aligned} \quad (41)$$

where we take $\Delta A_a(t) = H_{a1} F_1(t)E_a$, $\Delta B_a(t) = H_{a2} F_2(t)G_a$ and $\Delta C_a(t) = H_{a3} F_1(t)E_a$. One can verify that these matrices can be expressed as follows:

$$\begin{aligned} H_{a1} &= \begin{bmatrix} H_1 + B_2 D_{c2} H_3 \\ B_{c2} H_3 \end{bmatrix}, \quad H_{a2} = \begin{bmatrix} H_2 \\ 0 \end{bmatrix}, \quad H_{a3} = \tilde{D}_{c2} H_3, \\ E_a &= [E \ 0], \quad G_a = [G \ 0], \quad L_a = [L \ 0]. \end{aligned} \quad (42)$$

The robust H_∞ estimator for the coherent-classical system here is then obtained by solving two AREs of the form (23) and (24) with the relevant matrices as defined in (25). A suitable estimator is as defined in (26), (27).

Consider an example with the plant given by [8], [10]:

$$\begin{aligned} \begin{bmatrix} da \\ da^* \end{bmatrix} &= \begin{bmatrix} -\frac{\beta}{2} & -\chi \\ -\chi^* & -\frac{\beta}{2} \end{bmatrix} \begin{bmatrix} a \\ a^* \end{bmatrix} dt \\ &- \sqrt{\kappa_1} \begin{bmatrix} d\mathcal{A} \\ d\mathcal{A}^* \end{bmatrix} - \sqrt{\kappa_2} \begin{bmatrix} d\mathcal{U} \\ d\mathcal{U}^* \end{bmatrix}, \\ \begin{bmatrix} d\mathcal{Y} \\ d\mathcal{Y}^* \end{bmatrix} &= \sqrt{\kappa_1} \begin{bmatrix} a \\ a^* \end{bmatrix} dt + \begin{bmatrix} d\mathcal{A} \\ d\mathcal{A}^* \end{bmatrix}, \\ z(t) &= [0.1 \ -0.1] \begin{bmatrix} a \\ a^* \end{bmatrix}. \end{aligned} \quad (43)$$

Here, we choose $\beta = 4$, $\kappa_1 = \kappa_2 = 2$ and $\chi = -1$. Note that this system is physically realizable, since $\beta = \kappa_1 + \kappa_2$. The matrices in (35) may then be obtained.

The coherent controller (33) is of the form [8], [10]:

$$\begin{aligned} \begin{bmatrix} da_c \\ da_c^* \end{bmatrix} &= \begin{bmatrix} -\frac{\beta_c}{2} & -\chi_c \\ -\chi_c^* & -\frac{\beta_c}{2} \end{bmatrix} \begin{bmatrix} a_c \\ a_c^* \end{bmatrix} dt \\ &\quad - \sqrt{\kappa_{c1}} \begin{bmatrix} d\tilde{A} \\ d\tilde{A}^* \end{bmatrix} - \sqrt{\kappa_{c2}} \begin{bmatrix} d\mathcal{Y} \\ d\mathcal{Y}^* \end{bmatrix}, \\ \begin{bmatrix} d\tilde{Y} \\ d\tilde{Y}^* \end{bmatrix} &= \sqrt{\kappa_{c1}} \begin{bmatrix} a_c \\ a_c^* \end{bmatrix} dt + \begin{bmatrix} d\tilde{A} \\ d\tilde{A}^* \end{bmatrix}, \\ \begin{bmatrix} d\mathcal{U} \\ d\mathcal{U}^* \end{bmatrix} &= \sqrt{\kappa_{c2}} \begin{bmatrix} a_c \\ a_c^* \end{bmatrix} dt + \begin{bmatrix} d\mathcal{Y} \\ d\mathcal{Y}^* \end{bmatrix}. \end{aligned} \quad (44)$$

Here, we choose $\beta_c = 4$, $\kappa_{c1} = \kappa_{c2} = 2$ and $\chi_c = 0.5$. Note that this system is physically realizable since $\beta_c = \kappa_{c1} + \kappa_{c2}$. Then the matrices in (38) may be obtained.

We now consider the plant to be uncertain as in (36), (31) with $\alpha = \sqrt{\kappa_1}$ here. We set $\delta = -1$, $\mu = 0.1$ and fix the homodyne detection angle at 80° . Also, we choose $\gamma = 0.65$, $\epsilon_1 = 0.2$, $\epsilon_2 = 0.6$. A robust H_∞ purely-classical estimator is obtained as in (12), (37) with:

$$\begin{aligned} A_K &= \begin{bmatrix} 1.4589 + 1.4235\iota & -2.5630 - 0.2493\iota \\ -2.5630 + 0.2493\iota & 1.4589 - 1.4235\iota \end{bmatrix}, \\ B_K &= \begin{bmatrix} 0.8659 - 3.6066\iota \\ 0.8659 + 3.6066\iota \end{bmatrix}, C_K = [0.1 \quad -0.1]. \end{aligned} \quad (45)$$

Also, a robust H_∞ coherent-classical estimator is obtained as in (26) with:

$$\begin{aligned} A_{aK} &= \begin{bmatrix} -3.88 - 0.002\iota & 1.05 - 0.003\iota & -4.29 - 0.27\iota & 2.17 - 0.51\iota \\ 1.05 + 0.003\iota & -3.88 + 0.002\iota & 2.17 + 0.51\iota & -4.29 + 0.27\iota \\ -1.95 - 0.003\iota & 0.03 - 0.004\iota & -4.98 - 0.32\iota & 2.39 - 0.72\iota \\ 0.03 + 0.004\iota & -1.95 + 0.003\iota & 2.39 + 0.72\iota & -4.98 + 0.32\iota \end{bmatrix}, \\ B_{aK} &= \begin{bmatrix} 0.12 + 2.267\iota \\ 0.12 - 2.267\iota \\ 0.20 + 2.993\iota \\ 0.20 - 2.993\iota \end{bmatrix}, C_{aK} = [0.1 \quad -0.1 \quad 0 \quad 0]. \end{aligned} \quad (46)$$

Fig. 7 illustrates that the robust H_∞ coherent-classical filter provides with better disturbance attenuation compared to the robust H_∞ purely-classical filter for the uncertain plant. Fig. 8 shows that this holds for all values of δ . Moreover, we can see that the H_∞ norm for the robust coherent-classical estimator is uniform across the uncertainty window unlike the robust purely-classical estimator. That is, our robust coherent-classical estimator exhibits improved robustness to uncertainty as compared to the robust classical-only estimator. This is due to the coherent feedback involved here as opposed to the case of Fig. 4.

Note that we here considered uncertainty in B_1 only in (36). This is because any uncertainty in B_1 (and not B_2) in (35) will also cause C (besides A) to be accordingly uncertain owing to physical realizability constraints for our example (43). However, uncertainty in B_2 only and/or uncertainties in both B_1 and B_2 can be treated as well.

VI. CONCLUSION

In this paper, we studied robust H_∞ coherent-classical estimation, with and without coherent feedback, and compared with robust H_∞ purely-classical estimation for an uncertain linear quantum plant. We observed that our robust coherent-classical filter, whether or not involving coherent feedback,

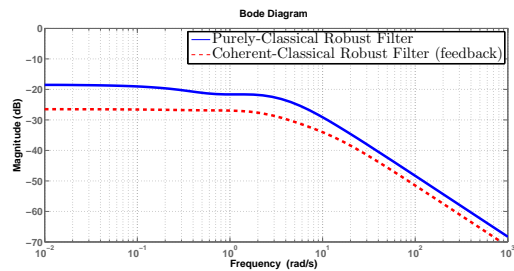


Fig. 7. Comparison of the estimation error frequency response of robust coherent-classical and robust purely-classical estimators.

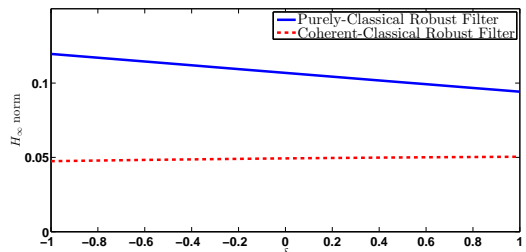


Fig. 8. Comparison of the H_∞ norm of the disturbance-to-error transfer functions for robust coherent-classical and robust purely-classical estimators.

can provide better disturbance attenuation than the purely-classical filter. Additionally, with coherent feedback, our robust coherent-classical filter provides superior robustness to uncertainty compared to the classical-only filter.

REFERENCES

- [1] H. M. Wiseman and G. J. Milburn, *Quantum Measurement and Control*. Cambridge University Press, 2010.
- [2] N. Yamamoto, "Robust observer for uncertain linear quantum systems," *Physical Review A*, vol. 74, p. 032107, 2006.
- [3] M. R. James, H. I. Nurdin, and I. R. Petersen, " H_∞ control of linear quantum stochastic systems," *IEEE Transactions on Automatic Control*, vol. 53, no. 8, pp. 1787–1803, 2008.
- [4] H. I. Nurdin, M. R. James, and I. R. Petersen, "Coherent quantum LQG control," *Automatica*, vol. 45, no. 8, pp. 1837–1846, 2009.
- [5] S. Lloyd, "Coherent quantum feedback," *Physical Review A*, vol. 62, p. 022108, 2000.
- [6] D. F. Walls and G. J. Milburn, *Quantum Optics*. Berlin; New York: Springer-Verlag, 1994.
- [7] C. Gardiner and P. Zoller, *Quantum Noise*. Berlin: Springer, 2000.
- [8] I. R. Petersen, "Coherent-classical estimation for quantum linear systems," in *Proceedings of the Australian Control Conference*, Perth, Australia, November 2013, pp. 371–376.
- [9] S. Roy, I. R. Petersen, and E. H. Huntington, "Coherent-classical estimation versus purely-classical estimation for linear quantum systems," in *Proceedings of the Conference on Decision and Control*, Los Angeles CA, USA, December 2014, pp. 5782–5787.
- [10] —, "Coherent-classical estimation for linear quantum systems," arXiv:1502.03729.
- [11] S. Roy and I. R. Petersen, "Robust H_∞ estimation of uncertain linear quantum systems," *International Journal of Robust and Nonlinear Control*, 2016, doi:10.1002/rnc.3530.
- [12] M. Fu, C. E. DeSouza, and L. Xie, " H_∞ estimation for uncertain systems," *International Journal of Robust and Nonlinear Control*, vol. 2, pp. 87–105, 1992.